ORIGINAL ARTICLE

European Journal of Soil Science WILEY

Responses of surface SOC to long-term experimental warming vary between different heath types in the high Arctic tundra

Ji Young Jung[1] | Anders Michelsen[2,3] | Mincheol Kim[1] | Sungjin Nam[1] |
Niels M. Schmidt[4] | Sujeong Jeong[1] | Yong-Hoe Choe[1] | Bang Yong Lee[1] |
Ho Il Yoon[1] | Yoo Kyung Lee[1]

[1]Korea Polar Research Institute, Incheon, South Korea

[2]Center for Permafrost (CENPERM), University of Copenhagen, Copenhagen, Denmark

[3]Department of Biology, University of Copenhagen, Copenhagen, Denmark

[4]Arctic Research Centre, Department of Bioscience, Aarhus University, Roskilde, Denmark

Correspondence
Yoo Kyung Lee, Korea Polar Research Institute, 26 Songdomirae-ro, Yeonsu-gu, Incheon 21990, Republic of Korea.
Email: yklee@kopri.re.kr

Abstract

Over the past few decades the Arctic has warmed up more than the lower latitudes. Soil organic carbon (SOC) in the Arctic is vulnerable to climate change, and carbon dioxide (CO_2) produced via SOC decomposition can amplify atmospheric temperature increase. Although SOC composition is relevant to decomposability, studies on its compositional changes with warming are scarce, particularly in the Arctic. Therefore, we investigated the responses of SOC and the bacterial community to climate manipulation under *Cassiope* and *Salix* heath vegetation communities in permafrost-affected soil in Zackenberg, Greenland. After 8–9 years of experimental warming, we evaluated changes in SOC quantity and quality of three density fractions of soil: free light fraction (FLF), occluded light fraction (OLF) and heavy fraction (HF). The SOC content at 0–5-cm depth was significantly reduced with warming under *Cassiope*, and it was accompanied by decreased FLF content, attributed to accelerated decomposition of the FLF by warming. However, SOC molecular composition and bacterial community composition were not affected by warming. By contrast, there was no warming effect on SOC under *Salix*, which could be partially due to smaller temperature increases caused by higher moisture levels associated with larger silt and clay contents, or to different responses of the dominant plant species to temperature. In both soils, more than 55% of SOC was associated with minerals, and its molecular composition indicated microbial decomposition. Our results suggested that long-term warming in the high Arctic could induce the loss of SOC, particularly in the FLF; however, the response could vary with vegetation type and/or soil properties, that is, soil texture.

Highlights

- We show decreased SOC with long-term (8-year) warming of heath soils in the high Arctic
- Particularly, the free light fraction of SOC in topsoil decreased with warming in a *Cassiope* heath site

- Mineral-associated SOC content was more than 55% and showed signs of microbial processing
- Effects of warming differed according to soil properties and/or plant community composition

1 | INTRODUCTION

Soils are the largest carbon (C) reservoir in terrestrial ecosystems. It is estimated that 1,035 Pg of C are stored in the upper 3 m of soils in permafrost regions (Hugelius et al., 2014). Greenhouse gases (i.e., carbon dioxide and methane) released from the active layer above the permafrost could feed back to the atmosphere to accelerate the global warming effect (Schuur et al., 2015). Because of the vulnerability of soil organic carbon (SOC) to climate change and the vast amount of SOC in the Arctic regions, the fate of SOC in response to climate warming is of great interest (Schuur et al., 2015). Furthermore, climate change in the Arctic is more pronounced than in other parts of the world (Huang et al., 2017). Therefore, it is important to understand the responses of arctic soils to climate change.

As temperatures increase, the contents of SOC decrease, increase or remain the same depending on the balance of C input to, and release from, the system (Crowther et al., 2016). Although increased plant biomass and litter input can lead to increases in SOC (Welker, Fahnestock, Henry, O'Dea, & Chimner, 2004), accelerated decomposition or decreased C input can lead to decreases in SOC with warming (Sjögersten, van der Wal, & Woodin, 2012). In contrast, other studies revealed that SOC content did not change with warming if newly added litter input compensated for the losses due to decomposition (Sistla et al., 2013; Xu, Sherry, Niu, Zhou, & Luo, 2012). Moreover, changes in temperature can lead to numerous indirect effects on litter input and decomposition, such as altered microbial community composition and activity, available nutrients and moisture content.

SOC fractionation can separate SOC pools with different mean residence times (Six et al., 2001; von Lützow et al., 2007). Many studies are based on either size- or density-based fractionation or combined methods. In soil density fractionation, the free light fraction (FLF) that floats on the surface of a dense solution is usually characterized as material similar to fresh plant residues with fast turnover rates. After removing the FLF, the remaining materials can be separated into the occluded light fraction (OLF) and heavy fraction (HF). The OLF is protected from microbial decomposition through physical barriers within soil aggregates and/or reduced oxygen availability. The HF that consists of mineral-associated organic matter with slow turnover rates is considered to be more stable and contains more microbially processed organic materials (Six et al., 2001). This SOC fractionation approach can help to capture the different responses among SOC pools to warming by allowing them to be investigated individually. When clear differences in changes in bulk SOC cannot be easily observed due to the cumulative effect of contrasting responses to environmental variables between different SOC fractions, these fractionation techniques can help to distinguish between the responses of different SOC pools (Guan et al., 2018; Xu et al., 2012).

The molecular composition of SOC can also be affected by warming irrespective of changes in SOC quantity. SOC characteristics are determined by the composition of plant litter or decomposed organic materials. When plant community composition is affected by warming (Xu et al., 2012), SOC composition can change because of the different chemistry of litter inputs. If the soil microbial community structure is altered by warming, this can also lead to changes in SOC composition (Wickings, Grandy, Reed, & Cleveland, 2012). For example, a decrease in the abundance of lignin-derived compounds in soil was associated with an increase in the abundance of fungi in response to soil warming (Feng, Simpson, Wilson, Dudley Williams, & Simpson, 2008). The molecular composition of SOC has been widely examined using ^{13}C-nuclear magnetic resonance (NMR) spectroscopy. Several studies showed that SOC stored in Arctic permafrost is composed of easily degradable and carbohydrate-rich materials (Mueller et al., 2015). Although labile SOC preserved by low temperatures in the Arctic is likely to be greatly affected by climate warming, the controls on SOC stability and stabilization mechanisms in Arctic soils are still unclear. Whereas Gentsch et al. (2015) reported mineral-associated SOC as a critical factor for long-term SOC stabilization in permafrost soils, Höfle, Rethemeyer, Mueller, and John (2013) showed that mineral association was relatively less important in the active layer as SOC associated with silt and clay minerals mainly comprised of recent plant input.

Therefore, SOC compositions and stabilization mechanisms are varied and should be investigated to determine the fate of SOC in a range of Arctic Cryosols exposed to current and future warming.

Although many studies have investigated quantitative changes in SOC in response to warming over short time periods, relatively few studies have focused on long-term responses to warming in the Arctic (Sistla et al., 2013; Sjögersten et al., 2012). Furthermore, only a handful of studies have examined SOC molecular compositions in the Arctic (Gentsch et al., 2015; Höfle et al., 2013; Mueller et al., 2015), and very few studies have related compositional changes in SOC fractions to warming in Cryosols (Guan et al., 2018; Xue et al., 2016). However, it is essential to investigate whether warming can induce changes in either SOC molecular composition or quantity, and whether changes in the soil microbial community that drive SOC turnover are related to the changes in SOC. Therefore, we investigated whether long-term experimental warming induced changes in SOC quantity under two common and widespread tundra heath types (*Cassiope* and *Salix*) found in different soil moisture conditions in the high Arctic. We also examined the mechanisms of the changes in SOC in response to warming through the analysis of bacterial community composition and biomass, density-based SOC fractionation and ^{13}C-NMR spectroscopic analysis of molecular composition of three SOC fractions (i.e., FLF, OLF and HF). We hypothesized that experimental warming would decrease the FLF and change the chemical composition of SOC because of increased litter input and accelerated decomposition. However, the warming effect on SOC would be more pronounced under a heath type in a drier condition with better drainage and higher oxygen availability.

2 | MATERIALS AND METHODS

2.1 | Site description

The study site was located at Zackenberg Research Station (74°30'N, 21°00'W), northeast Greenland. Annual mean temperature was −9.0°C and total precipitation ranged from 93 to 307 mm during 1996–2012 (Jensen & Rasch, 2013). The soil type was Turbic Cryosols (Arenic) in the FAO-WRB classification (IUSS Working Group WRB, 2015) and Typic Psammoturbels in the USDA system (Soil Survey Staff, 2014). The organic A horizon was 2–5 cm in depth and the B or B/C mineral horizon was subsoil (Elberling, Jakobsen, Berg, Søndergaard, & Sigsgaard, 2004). The permafrost was continuous and the active layer depths under *Cassiope* and *Salix* in the mid-August of 2012 were 80 and 60 cm, respectively. Climate manipulation plots were established in 2004 in two different heath types dominated by the evergreen dwarf shrub *Cassiope tetragona* or the deciduous dwarf shrub *Salix arctica*. Vascular plants, mosses

and lichen covered 65% and 80% of the ground at *Cassiope* and *Salix* sites, respectively (Elberling et al., 2004), and the rest of ground was covered with litter or bare soil. Whereas the *Cassiope* site also contained *Salix arctica* and *Vaccinium uliginosum*, the vegetation at the *Salix* site also comprised *Cassiope tetragona*, *Dryas* spp. and *Luzula arctica* (Campioli et al., 2013); see Elberling et al. (2004) for more information on the plant communities. There were five paired control and warming treatment plots (1 × 1 m^2) in each heath type. The control plots were marked with four long poles around the perimeter. Warming was simulated by erecting transparent 0.05-mm polyethylene film tents with an open top. The tent was installed at the beginning (mid-June) and removed at the end (end of August) of the vascular plant growing season each year. This operation was repeated during 2004–2012 for both heath types. Average soil temperatures from July 25 to August 13, 2007 at a depth of 3 cm were increased from 6.4 to 7.3°C under *Cassiope* and from 7.1 to 7.4°C under *Salix* by the warming treatment (Campioli et al., 2013).

2.2 | Litter and soil sampling

Soils under *Cassiope* and *Salix* were sampled in mid-August of 2011 and 2012, respectively. In each plot, three 15-cm-long soil cores with 5 cm diameter were randomly collected with a stainless-steel tube or a split tube sampler from an undisturbed area of the plot. The three cores were separated into the litter layer and 0–5, 5–10 and 10–15 cm depths, and pooled for the same depth. Field-moist soil samples were stored in a cooler and transported to the laboratory.

2.3 | Soil properties

The fresh weight of the pooled three soil cores that were 5 cm in length was measured and moisture content was determined after drying approximately 10 g of field-moist soil at 105°C (Table S1). Soil volume was measured based on the volume of the soil corer. Soil dry weight was calculated by using the moisture content of fresh soil. Soil bulk density was calculated by dividing soil dry weight by soil volume (Table S2). Visible roots were hand-picked, washed in a deionised water (DI) water bath, dried (45°C for 48 hr), and then weighed (Table S3). Soil was air-dried and sieved through a 2-mm sieve before further analyses. To determine soil texture, soil was treated with concentrated hydrogen peroxide to remove organic materials. Soil was mixed with 5% sodium hexametaphosphate solution and shaken for 18 hr. The proportion of sand was acquired after wet-sieving through a 53-μm sieve (Gee & Or, 2002), and that of silt and clay was determined using Micromeritics Sedigraph 5120 (Micromeritics, Norcross, GA, USA). Soil pH was determined in water by a 1:2 (w/v) ratio (Table S4). Soil was

finely ground with a ball mill for analysing total carbon (TC) and nitrogen (TN). Total C and TN contents were measured by a combustion method at 950°C with an elemental analyser (FlashEA 1112; Thermo Fisher Scientific, Waltham, MA, USA). The total inorganic carbon (TIC) content was determined by the amount of carbon dioxide (CO_2) produced from a reaction of powdered soil and phosphoric acid at 80°C with a CO_2 coulometer (CM5014; UIC Inc., Joliet, IL, USA). Because the TIC content was less than 0.003% in all samples, the TC content was considered as the SOC content. The SOC stock was calculated using Equation 1:

$$SOC\ stock = \sum\nolimits_{i=1}^{3} SOCcon_i \times \rho_i \times depth_i, \qquad (1)$$

where $SOCcon_i$ is the content of SOC for depth i, ρ is the soil bulk density, and $i = 1$ for 0–5 cm, $i = 2$ for 5–10 cm and $i = 3$ for 10–15-cm depth of soil.

Density-based fractionation of SOC was conducted according to the method described by Six et al. (2001) and Paré and Bedard-Haughn (2011), with some modifications. Five grams of soil and 30 mL of sodium polytungstate (SPT, 1.55 g cm^{-3}) solution were mixed. Floating material was collected through centrifugation and vacuum filtration through a muffled class microfiber (GF/A) filter; this fraction was the FLF. The remaining material was again mixed with 30 mL of sodium polytungstate (1.55 g cm^{-3}) and sonicated (VCX-500 with a 13-mm solid end type probe; SONICS, Newtown, CT, USA) in an ice bath at a rate of 200 J mL^{-1} to disrupt aggregates and to release the occluded organic materials. The output of ultrasonic energy was calibrated by temperature change in water during sonication. The solution was again centrifuged, and the floating materials, comprising the OLF, were collected through vacuum filtration. The remaining HF was rinsed with DI water three times to remove the remnant sodium polytungstate. All three fractions were dried at 45°C, weighed and finely ground. The TC and TN contents from each fraction were measured as described above. Mass, C and N recovery of the fractionation method were 99.1 ± 1.0%, 96.0 ± 22.5% and 98.4 ± 23.5%, respectively.

2.4 | ^{13}C CPMAS NMR spectroscopic analysis of topsoil

Three of the five replicate samples were randomly selected and analysed using solid-state ^{13}C cross-polarization and magic-angle spinning nuclear magnetic resonance spectroscopy (^{13}C CPMAS NMR); the reduction in replication was due to the high cost of analysis. Additional NMR analyses were performed for the remaining two samples when significant differences were detected between the initial three replicate samples to strictly verify the significance. The finely ground FLF, OLF and HF of the topsoil (0–5 cm in depth) were used for ^{13}C

CPMAS NMR analysis. Prior to the NMR analysis, the HF was treated with 10% hydrofluoric acid to remove paramagnetic species and minerals. The ^{13}C NMR spectra were acquired with an Avance II+ Bruker Solid-state NMR spectrometer (Bruker Corporation, Billerica, MA, USA) at the Korea Basic Science Institute, Seoul Western Center, South Korea, operating at a ^{13}C Larmor resonance frequency of 100.62 MHz. Samples were confined in a zirconium oxide rotor with an external angle spinning technique applied with a contact time of 2 ms, a spinning rate of 12 kHz and a pulse delay of 3 s. The downfield C resonance peak of adamantine of 38.3 ppm at room temperature was used as an external chemical shift reference. The acquired spectra were integrated over the chemical shift ranges of 0–45 ppm (alkyl C), 45–110 ppm (O/N alkyl C), 110–160 ppm (aromatic C) and 160–220 ppm (carboxyl C). We analysed the ^{13}C NMR spectra using the procedure described by Eldridge et al. (2013) to characterize molecular composition (i.e. carbohydrate, protein, lignin, aliphatic compounds, carbonyl compounds and charcoal in the samples) (Table S5).

2.5 | Soil bacterial community analysis

We examined the warming effect on soil bacteria by comparing abundance, diversity and structure of bacterial communities in the litter layer, and 0–5 and 5–10-cm soil depths (but not the 10–15-cm depth) of the control and warmed plots. Bacterial abundance was estimated by quantifying bacterial 16S rRNA gene copies, and the composition and diversity of bacterial communities were analyzed using 16S rRNA gene amplicon sequencing. A small portion of samples in the litter layer and fresh soil was mixed with RNAlater solution (Life Technology, Carlsbad, CA, USA) and kept at 4°C in the laboratory in Zackenberg and transported to Korea for further analysis. Soil DNA was extracted from 0.3 g of each litter and soil sample using a FastDNA® SPIN Kit (MP Biomedicals, Santa Ana, CA, USA) according to the manufacturer's protocol. Two-step PCR was performed with the first step on the bacterial 16S rRNA gene (V3–V4 region) using primers 341F/785R (Klindworth et al., 2013), followed by the second index PCR according to the guidelines of Illumina MiSeq library preparation for 16S amplicon sequencing. Purified PCR products were sequenced using Illumina MiSeq (2 × 300 bp) at Macrogen (Seoul, Korea). Initial quality filtering was carried out following the quality-score-based error removal strategy suggested by Schirmer et al. (2015), with the combination of quality trimming (Sickle) and error correction (BayesHammer). Quality-trimmed paired end reads were merged using PANASeq v2.9 with a minimum overlap of 10 bp. The resultant reads were further processed following the MiSeq SOP in mothur v1.39.0 (Schloss et al., 2009). The chimera was detected using the de novo UCHIME algorithm, and sequences were classified by

matching them against the EzTaxon-e database using the naïve Bayesian classifier with a confidence threshold of 80%. The resultant high-quality sequences were clustered into operational taxonomic units (OTUs) at 97% similarity cut-off and singleton OTUs were removed. Raw sequencing data were submitted to the NCBI Sequence Read Archive (SRA) with accession number PRJNA416693.

Quantitative PCR (qPCR) assays for the bacterial 16S rRNA gene using the extracted DNA from litter and soil samples (0–5 and 5–10-cm depths) were performed on a CFX96 qPCR system (Bio-Rad, Hercules, CA, USA) with SYBR Green as the fluorescent reporter (Bio-Rad) in order to quantify the bacterial communities among different treatments. Partial bacterial 16S rRNA genes were amplified using primers 341f (5'-CCTACGGGAGGCAGCAG-3′) and 797r (5'-GGACTACCAGGGTCTAATCCTGTT-3′). Amplification was performed in triplicate with 44 cycles of denaturation at 94°C for 10 s, annealing at 64.5°C for 25 s and extension at 72°C for 25 s. Standard curves were generated using a tenfold dilution series of plasmids containing bacterial 16S rRNA genes obtained from soil samples. No template control (NTC) was also run in triplicate for negative control.

2.6 | Statistical analysis

Normality and equal variance assumptions for all data were tested before data analyses. Pairwise *t*-tests were used for soil properties data analysis to compare mean differences between control and warming treatments ($p < .05$). If either of the two assumptions above was violated, data were log-transformed. If the transformed data still did not meet the assumptions, a non-parametric method (Wilcoxon signed ranks method) was used

to test the warming effect. For microbial community analysis, a Hellinger-transformed OTU matrix was used to calculate Bray-Curtis dissimilarities between samples, and principal coordinates analysis (PCoA) was used for ordination analysis. The level of bacterial diversity, calculated by the Shannon index (H'), was compared between different samples after standardizing reads to the smallest library size ($n = 3,685$). To test for significant differences in bacterial community structure between different groups (i.e., vegetation type, soil depth, and treatment), a permutational multivariate analysis of variance (PERMANOVA) was performed with 999 permutations using PRIMER v6 and PERMANOVA+. All statistical analyses were performed using JMP 11.0 (SAS Institute Inc., Cary, NC, USA) and R Statistical Software (version 3.0.1; R Foundation for Statistical Computing, Vienna, Austria).

3 | RESULTS

3.1 | Soil properties

Soil texture of the two heath types was different. *Cassiope* heath soil was a sandy loam containing a high percentage of sand, whereas *Salix* heath soil was a clay loam with high silt and clay percentages (Table 1). Particle size distribution was significantly different between warming and control plots in *Cassiope* heath soil at 5–10-cm depth (Table 1, $p < .05$). At this depth, the sand fraction was significantly higher in the warming plots, whereas the silt and clay fractions were significantly lower than those in control plots under *Cassiope*.

Root weight density (RWD) in *Salix* heath plots was higher than that in *Cassiope* heath plots and decreased with depth (Table S3). The RWD was not different between

TABLE 1 Soil texture in control and warming plots in *Cassiope* and *Salix* heaths

| Soil depth (cm) | | Cassiope | | | | Salix | | | |
| | | Control | | Warming | | Control | | Warming | |
		Mean	SD	Mean	SD	Mean	SD	Mean	SD
0–5	Sand (%)	62.1	10.0	61.8	8.6	22.5	12.6	21.7	9.5
	Silt (%)	26.9	9.2	26.8	8.2	43.4	9.4	42.3	6.5
	Clay (%)	11.0	1.0	11.4	1.4	34.1	3.6	36.0	5.8
5–10	Sand (%)	63.8	6.7	73.0	10.4 (.039)	22.0	12.7	21.5	9.4
	Silt (%)	24.1	6.7	17.4	7.9 (.042)	44.2	8.2	44.2	4.7
	Clay (%)	11.7	1.4	9.6	2.6 (.034)	33.8	4.8	34.3	5.4
10–15	Sand (%)	65.4	10.4	74.7	12.6	22.6	12.9	21.5	10.4
	Silt (%)	23.6	8.3	16.5	10.2	44.2	9.2	43.5	6.1
	Clay (%)	11.0	2.7	8.8	3.2	33.2	4.1	35.0	5.3
Texture		Sandy loam				Clay loam			

Note: Differences between control and warming plots were analysed by pairwise *t*-test. *p*-value is reported in brackets in the case of $p \le .05$.
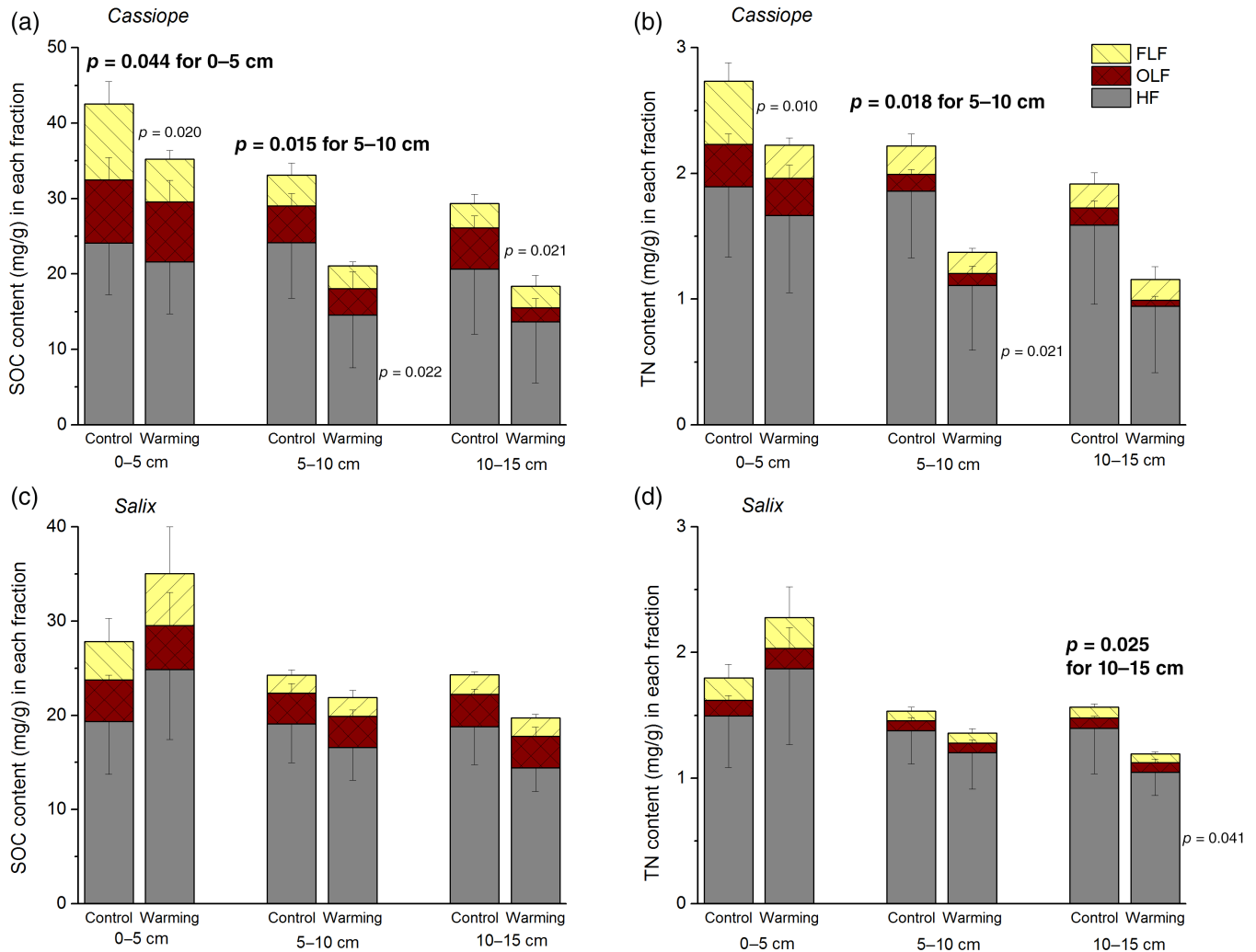Abbreviation: SD, standard deviation ($n = 5$).

FIGURE 1 Soil organic carbon (SOC) and total nitrogen (TN) contents at 0–5, 5–10 and 10–15-cm depth in *Cassiope* and *Salix* heaths. The pools of C and N in the free light fraction (FLF, light yellow colour with a diagonal line pattern), occluded light fraction (OLF, brown colour with a cross-diagonal pattern) and heavy fraction (HF, grey colour with no pattern) following density fractionation at 0–5, 5–10 and 10–15-cm depth are shown in different colours and patterns of each bar. Differences between control and warming plots were analysed by pairwise *t*-test or the Wilcoxon singed ranks method when normality was violated. The *p*-value is reported in cases of $p \leq .05$. The bold *p*-value on the top of the bar graphs shows significant difference in C or N content of bulk soil between control and warming, and the *p*-value on the right side of the bar graphs means significant difference in C or N content of each fraction between control and warming. Means and standard deviations (SDs, $n = 5$) are reported [Color figure can be viewed at wileyonlinelibrary.com]

control and warming treatments in both heath types, but the mean value was lower and higher in warming plots for depth of 0–5 cm under *Cassiope* and *Salix*, respectively (Table S3).

The SOC contents for depths of 0–5 and 5–10 cm under *Cassiope* were significantly lower than the control after 8 years of warming (Figure 1a, $p < .05$), whereas there were no significant differences under *Salix* after 9 years of warming. The SOC and TN contents in *Cassiope* heath plots were higher than those in *Salix* heath plots. The SOC contents sharply decreased with depth under *Cassiope*, but the variation between depths was not large under *Salix* (Figure 1a, c).

The weight-based relative proportion of FLF at 0–5-cm depth in warming plots under *Cassiope* was 2.2% and was significantly lower than that in control plots (Figure S1, $p < .05$). The FLF-C content at 0–5-cm depth, the HF-C content at 5–10-cm depth and the OLF-C content at 10–15-cm depth were significantly lower under warming than in the control at the *Cassiope* site (Figure 1a). Because the C and N contents and C/N ratios of the FLF were not different between control and warming treatments under both heath types (Table 2, $p > 0.05$), decreased FLF-C content with warming was mainly attributed to the lower mass proportion of FLF at 0–5-cm depth under *Cassiope*. The FLF-N, OLF-N and HF-N contents showed the same trend as C

TABLE 2 Total C and N contents in the free light fraction (FLF), occluded light fraction (OLF) and mineral-associated heavy fraction (HF) following density fractionation of soil at 0–5, 5–10 and 10–15-cm depths in *Cassiope* and *Salix* heath

Soil depth (cm)		*Cassiope*				*Salix*			
		Control		Warming		Control		Warming	
		Mean	SD	Mean	SD	Mean	SD	Mean	SD
FLF									
0–5	C (mg g^{-1})	315.0	11.3	317.7	23.8	241.4	37.9	262.7	47.2
	N (mg g^{-1})	13.9	1.5	14.6	1.1	11.0	2.1	12.1	2.2
	C/N ratio	22.9	2.5	21.8	0.6	22.2	2.7	21.8	1.1
5–10	C (mg g^{-1})	283.2	16.9	281.9	16.1	243.0	26.0	255.0	18.9
	N (mg g^{-1})	14.4	1.4	14.4	0.8	10.8	1.8	11.0	1.0
	C/N ratio	19.7	1.1	19.6	1.4	22.8	2.9	23.3	1.2
10–15	C (mg g^{-1})	266.5	29.7	287.4	8.7	256.6	34.4	258.5	27.5
	N (mg g^{-1})	13.6	1.8	15.9	2.0	12.1	2.9	10.8	1.8
	C/N ratio	19.8	1.5	18.2	1.9	21.6	2.5	24.4	4.3
OLF									
0–5	C (mg g^{-1})	409.9	21.9	416.3	6.9	438.8	18.3	441.5	22.3
	N (mg g^{-1})	15.0	1.5	15.1	0.9	13.4	2.2	14.3	1.8
	C/N ratio	27.6	3.7	27.5	1.4	33.5	6.2	31.4	5.0
5–10	C (mg g^{-1})	444.7	13.2	348.8	126.1	462.4	29.7	482.7	20.2
	N (mg g^{-1})	11.3	1.0	8.7	2.8	12.2	1.0	12.6	0.5
	C/N ratio	39.6	4.6	39.8	4.4	38.3	4.5	38.3	2.5
10–15	C (mg g^{-1})	454.9	26.9	313.4	154.1	454.9	36.1	504.6	21.4 (.037)
	N (mg g^{-1})	9.6	0.4	7.4	3.6	12.3	0.8	12.9	1.4
	C/N ratio	47.2	3.5	40.8	7.3	36.9	2.6	39.5	2.7
HF									
0–5	C (mg g^{-1})	27.5	6.4	27.3	6.6	16.5	3.6	18.6	3.6
	N (mg g^{-1})	1.9	0.5	2.0	0.5	1.4	0.3	1.5	0.3
	C/N ratio	14.5	2.0	13.5	1.0	12.1	0.7	12.2	0.8
5–10	C (mg g^{-1})	21.5	5.9	14.8	5.5 (.039)	16.3	3.5	14.9	2.6
	N (mg g^{-1})	1.6	0.5	1.1	0.5	1.3	0.3	1.2	0.2
	C/N ratio	14.1	1.2	14.2	1.3	12.2	0.6	12.0	0.4
10–15	C (mg g^{-1})	19.2	6.2	13.6	6.2	16.5	3.2	13.0	2.3 (.042)
	N (mg g^{-1})	1.3	0.4	0.9	0.4	1.4	0.3	1.1	0.2
	C/N ratio	14.6	0.8	14.5	1.5	12.1	0.1	11.9	0.3

Note: Differences between control and warming plots were analysed by pairwise *t*-test or the Wilcoxon singed ranks method when normality was violated; *p*-value is reported in brackets in the case of $p \leq .05$.

Abbreviation: SD, standard deviation ($n = 5$).

(Figure 1b). The FLF-N content at 0–5-cm depth and the HF-N content at 5–10-cm depth were significantly lower under warming than in the control at the *Cassiope* site (Figure 1b). Although SOC and TN contents with warming under *Salix* were lower than those in the control for the 10–15-cm depth, all FLF-C, OLF-C and HF-C contents did not differ between control and warming treatments (Figure 1c, d).

The FLF-C, OLF-C and HF-C contents contributed to the total SOC content for the 0–5-cm depth as 24, 20 and 56%, respectively, under *Cassiope* (Figure 1a). The contribution of the HF to the TN content (69–83%) was higher than the C contribution from the HF to the total SOC (56–72%) under *Cassiope* (Figure 1a, b). The HF-N content was higher than the FLF-N and OLF-N contents under both heath types
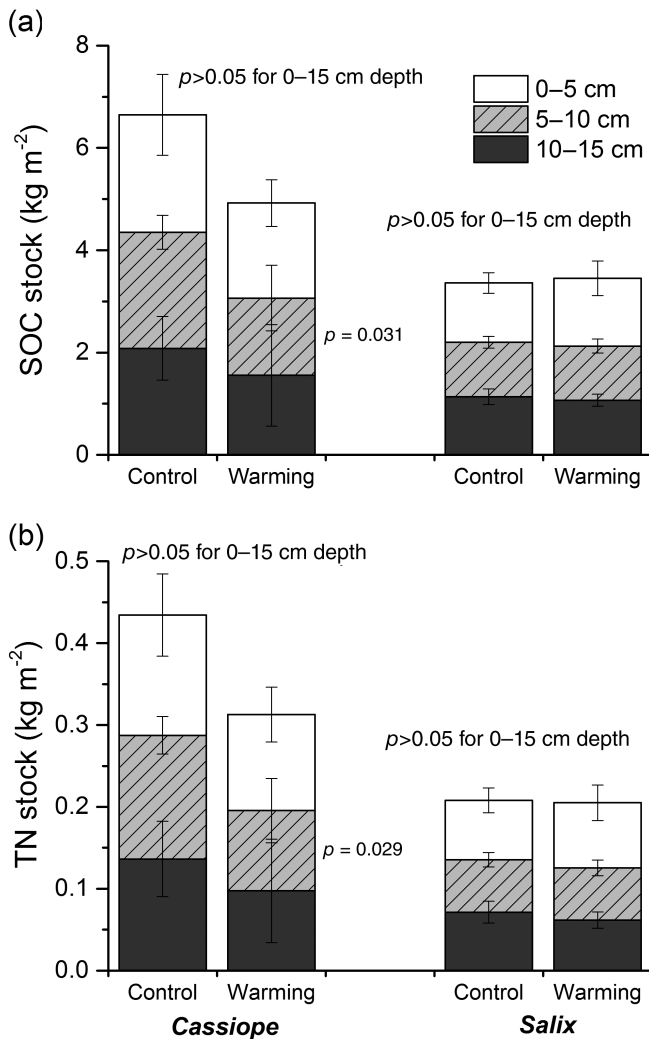
FIGURE 2 Soil organic carbon (SOC) and total nitrogen stock at 0–5, 5–10 and 10–15-cm depth in *Cassiope* and *Salix* heaths. Differences between control and warming plots were analyzed by pairwise *t*-test or the Wilcoxon singed ranks method when normality was violated. The *p*-value is reported in cases of $p \leq .05$. The *p*-value on the top of the bar graphs shows no significant difference in SOC or total nitrogen (TN) stock for the 0–15-cm depth between control and warming, and the *p*-value on the right side of the bar graphs means significant difference in SOC or TN stock at each depth between control and warming. Means and standard deviations (SDs, $n = 5$) are reported

(Figure 1b, d). In the *Salix* plots, C and N contributions of the HF to the overall content were higher than those in *Cassiope* plots (Figure 1c, d). Overall, more than 55% of SOC and TN was mineral associated in both heath types.

The SOC stocks under *Cassiope* for the 0–15-cm depth in control and warming plots were 6.64 ± 1.31 and 4.92 ± 1.82 kg C m^{-2}, respectively, although the difference between treatments was not significant (Figure 2, $p = .13$). However, the SOC stock at the 5–10-cm depth under *Cassiope* was significantly lower in the warming plot than in

the control (Figure 2, $p < .05$). The TN stock under warming was also lower than that in the control for the 0–5-cm and 5–10-cm depths; however, the difference of the TN stock for the 0–15-cm depth was not significant ($p = .086$) under *Cassiope*. The SOC and TN stocks under *Salix* did not vary with warming, and the SOC and TN contents did not either (Figure 2).

3.2 | ^{13}C CPMAS NMR spectroscopic analysis of topsoil

Relative proportions of C functional groups in all fractions did not show any significant differences between the topsoils under warming and control treatments in both *Cassiope* and *Salix* heath sites (Table 3 and Figure S2). When the two heath types were compared, the proportion of the alkyl group was higher and that of the aromatic group was lower in the *Cassiope* than in the *Salix* heath soil. Among the four functional groups, the proportion of the O/N alkyl group was the highest in all three fractions of *Cassiope* soil. For *Salix* soil, whereas the O/N alkyl group constituted the highest proportion of C functional groups in the FLF and HF, the aromatic group was predominant in the OLF (Table 3).This accounted for the highest proportion of coal/ charcoal in the OLF under *Salix* (Table S5).

3.3 | Soil and litter bacterial community analysis

The number of bacterial 16S rRNA gene copies in this region ranged from 3.3×10^5 to 6.9×10^8 per gram of dry soil. Bacterial abundance declined with increasing soil depth in the *Cassiope* sites, whereas the abundance was relatively constant throughout depths in the *Salix* sites (Figure 3). In both vegetation sites, bacterial diversity was higher in the litter layer than in the lower-depth (0–5 cm and 5–10 cm) soils (*t*-test, all $p < .05$, Figure 3). However, there were no significant warming effects on bacterial abundance or diversity (*t*-test, all $p > .05$). The PCoA analysis revealed that bacterial communities were grouped mainly by vegetation type and soil depth (PERMANOVA, all $p < .001$, Figure 4 and Table S6). There was no significant difference in bacterial community composition between warming and control at any depth (PERMANOVA, all $p > .05$, Figure 4).

4 | DISCUSSION

4.1 | Different soil responses to warming between *Cassiope* and *Salix* heath sites

A substantial decrease in SOC pools with warming was found in the *Cassiope* plots but not in the *Salix* plots

| | | Cassiope | | | | Salix | | | |
| | | Control | | Warming | | Control | | Warming | |
		Mean	SD	Mean	SD	Mean	SD	Mean	SD
FLF	Alkyl	28.4	2.3	29.5	3.7	18.0	1.5	18.7	2.7
	O/N alkyl	50.8	2.7	49.2	2.0	56.5	3.7	57.0	3.4
	Aromatic	12.4	1.0	12.7	1.6	17.7	2.8	17.2	3.0
	Carboxyl	8.4	0.4	8.7	0.4	7.9	0.9	7.1	0.5
OLF	Alkyl	39.9	1.7	39.5	1.3	27.3	1.8	28.2	3.0
	O/N alkyl	43.3	2.3	42.9	0.9	31.1	7.7	27.5	5.5
	Aromatic	10.1	0.8	10.5	0.9	34.0	10.0	36.0	8.0
	Carboxyl	6.7	1.0	7.1	0.5	7.6	1.2	8.2	0.7
HF	Alkyl	31.4	1.2	30.2	0.6	27.0	1.3	26.4	1.3
	O/N alkyl	48.3	0.9	49.0	1.8	48.5	2.1	48.6	1.4
	Aromatic	10.3	0.6	10.6	0.8	14.8	2.1	15.2	1.7
	Carboxyl	10.0	0.4	10.3	0.5	9.7	0.7	9.7	0.8

TABLE 3 Relative proportions of C functional groups in the three density fractions: free light fraction (FLF), occluded light fraction (OLF) and mineral-associated heavy fraction (HF) of topsoil (0–5 cm) under different tundra heath types

Note: Soils for the 0–5-cm depth were used. Differences between control and warming plots were analysed by pairwise *t*-test or the Wilcoxon singed ranks method when normality was violated. *p*-value was greater than 0.05 in all comparisons.

Abbreviation: SD, standard deviation ($n = 5$ for the FLF and HF of *Cassiope* soil; $n = 3$ for the rest).

(Figures 1 and 2). This could be mainly attributed to different temperature increases between the two plots despite the same warming simulation through transparent film tents. Although we do not have data for temperature changes during the whole manipulation period, Campioli et al. (2013) reported an average 0.9 and 0.3°C increase in warmed soil at 3-cm depth under *Cassiope* and *Salix*, respectively, from the end of July to mid-August in 2007 in the same experimental plots. The lower degree of soil temperature increase in *Salix* compared to *Cassiope* plots may have moderated responses in SOC quantity and quality. Different temperature responses could also originate from differences in water holding capacity of the soil, as soil texture in the *Cassiope* and *Salix* sites was sandy loam and clay loam, respectively (Table 1). Although we did not measure soil moisture differences in the experimental plots, Elberling et al. (2004) showed higher volumetric soil moisture content at 5-cm depth under *Salix* than under *Cassiope* at the same experimental sites. Therefore, soil under *Salix* with clay loam soil was likely to hold water more than that in the sandy loam under *Cassiope*, leading to less increase in soil temperature in the *Salix* plots due to the higher specific heat capacity of water than of air in soil pore spaces. Sjögersten et al. (2012) reported that a warming effect on SOC content was only significant in a mesic site but not in a wet one. Alatalo, Jägerbrand, Juhanson, Michelsen, and Ĺuptáčik (2017) also found SOC and TN loss with warming only in the mineral layer of mesic meadow but not from the organic layer of mesic meadow or both layers of soil in a wet meadow.

Although they did not explicitly mention the differences in the increase in temperature, both studies underscore the importance of soil moisture conditions for decomposition of SOC. Furthermore, because the SOC decomposition rate was slow in soils with high clay contents (Xu et al., 2016), the higher clay contents in the *Salix* plots may retard the responses to warming relative to the sandy loam soil of the *Cassiope* plots.

The biomass of leaves produced in a year compared to the total aboveground biomass, that is, relative growth rate (RGR) of *Salix*, was not affected by the warming treatment (Campioli et al., 2013), potentially contributing to the lack of effects on SOC quantity and quality under *Salix*. Compared to no changes in aboveground growth rate and biomass in the *Salix* plots with warming, the RGR of *Cassiope* under warming was approximately doubled, and it was consistent with increases in the number of branches and photosynthesis (i.e., gross ecosystem production, GEP) (Campioli et al., 2013). However, there were no significant changes in root biomass in either species (Table S3). The aboveground plant responses might be related to characteristics that are more responsive to temperature change in *Cassiope* than in *Salix*. *Cassiope* growth was strongly correlated with summer temperature in many chronological studies (Rozema et al., 2009), whereas this was not the case for *Salix arctica* (Schmidt, Baittinger, & Forchhammer, 2006). Thus, soil properties, that is, soil texture, could have an impact on the degree of on-site warming, and the responses to increased temperature also depend on the characteristics of the
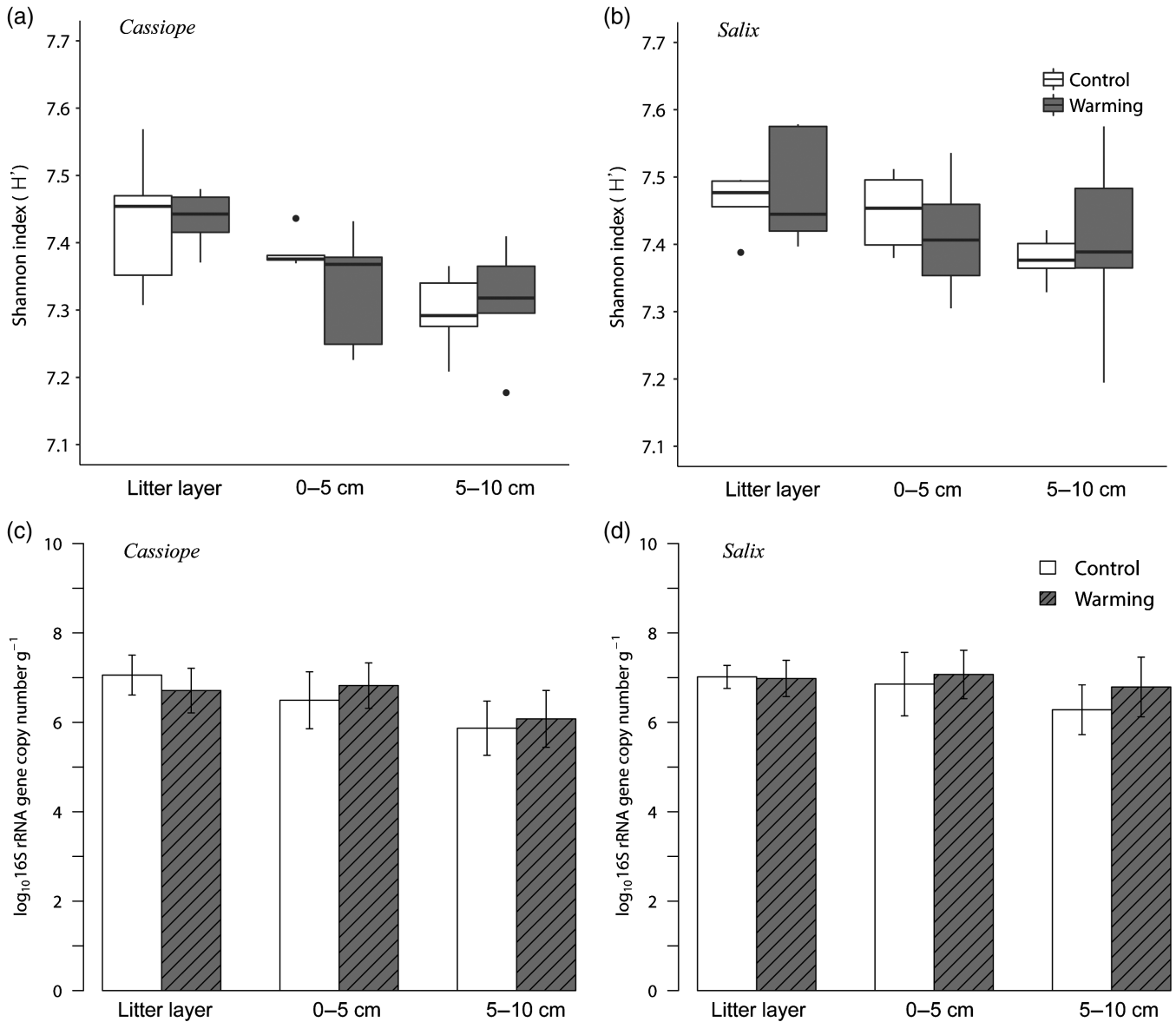
FIGURE 3 Bacterial diversity and abundance in the litter layer and in the 0–5 and 5–10-cm soil depths in *Cassiope* and *Salix* heaths. The top panels, (a) and (b), are boxplots of the Shannon diversity index, and the bottom panels, (c) and (d), represent means and standard deviations ($n = 5$) for bacterial 16S rRNA gene copy number. *p*-value was greater than .05 in all comparisons

dominant plant species. In addition to temperature increases, the effects of the warming tents on other parameters such as light penetration, soil moisture and wind might also have influenced the different responses of the soils in the control and treatment plots of the *Cassiope* and *Salix* heath sites.

4.2 | Responses of SOC to warming: quantity and quality

The SOC content decreased after 8 years of warming under *Cassiope*, and this decrease was mainly caused by the decrease in the quantity of FLF in the top 5-cm soil depth (Figure 1 and Figure S1). Many field-based experiments demonstrated a

decrease in SOC content after warming (Alatalo et al., 2017). Some warming experiments demonstrated a decrease in light fractions despite no significant changes in the bulk SOC content or in the C content in the HFs (Xu et al., 2012). The decreased FLF content under warming in the *Cassiope* heath soil observed in our study was consistent with that of previous studies. However, the decreased SOC content in our study indicated that the degree of decomposition was greater than the C input in soil despite increased RGR and GEP in *Cassiope*, as previously shown by Campioli et al. (2013) in this ecosystem. Increased GEP with warming was a general response in many warming experiments in tundra ecosystems; however, SOC could decrease (Biasi et al., 2008) or show no change
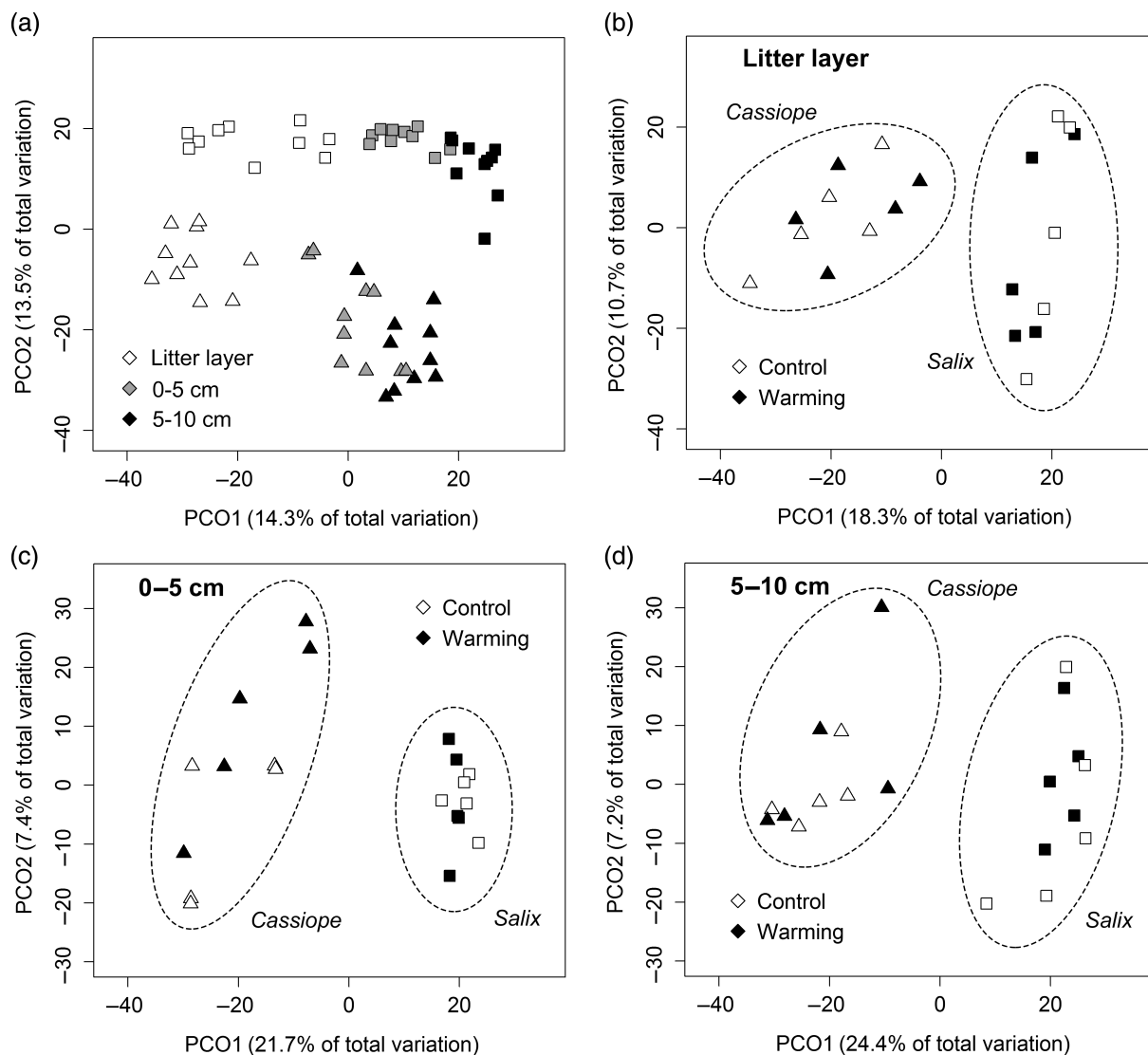
FIGURE 4 Principal coordinates analysis (PCoA) of bacterial community structure for (a) the whole dataset and warming effect at different soil depths, (b) litter layer, (c) 0–5 cm and (d) 5–10 cm. Operational taxonomic unit (OTU) abundance matrices were used to calculate Bray-Curtis dissimilarities between samples. Triangles represent *Cassiope* sites and squares indicate *Salix* sites

(Guan et al., 2018; Zhang, Shen, & Fu, 2015). These differential effects of responses to warming on SOC shown in several studies could be explained by numerous abiotic and biotic controls on soil attributes associated with warming. In addition, the mass contribution of the FLF to the total soil mass was less than 5%; however, its contribution to SOC content was approximately 20% at the 0–5-cm depth (Figure 1a and Figure S1). We only observed a significant decrease in FLF content at the 0–5-cm depth at the *Cassiope* site; however, this change was noteworthy because a change in FLF content could be associated with a change in the HF (Thaysen, Reinsch, Larsen, & Ambus, 2017) through C transfer from the FLF to HF (Schrumpf et al., 2013).

The reduction in the SOC stock and content by warming was most pronounced and statistically significant at the

5–10-cm depth under *Cassiope* (Figures 1 and 2). The SOC content with warming in the HF was markedly and significantly lower than in the control at the 5–10-cm depth (Table 2). This could be attributed to soil textural difference; sand content was 10% higher, and silt and clay content was lower in warming plots compared to the control at the 5–10 cm depth under *Cassiope*. The coarser particles generally contain less C than the finer particles owing to the decrease of specific surface areas and reactive sites for SOC–mineral association with increasing particle size (Xu et al., 2016). On the other hand, more sand content under warming plots could cause faster SOC decomposition with better drainage and higher oxygen availability. Comparing SOC after 8 years of warming with soils collected before the experiment was set up at the same spots would be

ideal to confirm the warming effect by eliminating possibilities from prior textural differences due to random effects. However, we do not have the baseline soil samples and this is the major caveat in this study, and in the majority of similar studies on C stocks in response to warming. We encourage scientists in this field to consider the necessity of baseline sampling prior to experimental manipulations.

The calculated loss of the SOC stock with warming only for the 0–5-cm depth, excluding the other depths, was 0.44 kg C m^{-2} over 8 years of manipulation periods (i.e., 54.5 g C m^{-2} yr^{-1}). The modelled net ecosystem exchange (NEE) of CO_2 and ecosystem respiration (ER) were estimated at -15 ± 10 and 78 ± 9 g C m^{-2} yr^{-1} under the *Cassiope* heath ecosystem in Zackenberg, NE Greenland (Zhang et al., 2018). Our measured SOC loss due to warming, thus, seems to be high compared to the previous reported values of NEE and ER in the *Cassiope* heath (Zhang et al., 2018). This calculation assumed no decrease in the amount of C input to the soil. However, several studies showed an increased aboveground/belowground allocation ratio with increased temperature in tundra, because warming increased light competition or nutrient availability (Wang et al., 2016). If the increased GEP only contributed to increase aboveground but not belowground production, the C input from the belowground part might be reduced with warming. Although it was not statistically significant, the root biomass of *Cassiope* for the 0–5-cm depth was lower in the warming treatment than in the control (Table S3). Thus, reduced C input in soil might be one reason for the reduced SOC content associated with warming under *Cassiope*. Moreover, SOC decomposition is a part of SOC loss, and DOC leaching, which differs between contrasting soil textures, can be another pathway of SOC loss (Guo, Ping, & Macdonald, 2007) that was not included in the C budget described by Zhang et al. (2018). Furthermore, warming can increase root exudation, which can promote SOC decomposition through a priming effect (Wild et al., 2016). Although DOC was not affected by warming, a parallel study that focused on litter decomposition in our plots (Blok et al., 2018) showed that litter mass loss was greater in warmed plots, and that total dissolved N and ammonium in the soil was lower in both heath types, possibly due to enhanced plant uptake in response to warming. The relative importance of DOC and respiration as pathways of C losses from different high arctic heath ecosystems should be a focus in future studies.

In contrast to the significant decrease in SOC content with warming under *Cassiope*, SOC molecular composition was unaltered in both tundra heath types (Table 3 and Figure S2). Although the FLF content, which contains about 50% of O/N alkyl groups, decreased, the relative abundance of this group did not show any differences between treatments (Figure 1 and Table 3). The O/N alkyl group represents the major components of the FLF as polysaccharides (i.e., cellulose, hemicellulose) (Kögel-Knabner, 1997). Although there are reports of significant changes in SOC molecular composition with warming (Feng et al., 2008; Pisani et al., 2014), other studies did not find any differences in SOC molecular composition with warming in either forest or alpine ecosystems (Schnecker, Borken, Schindlbacher, & Wanek, 2016; Zhao et al., 2018). This was consistent with the lack of change in SOC molecular composition in our study. The increased soil temperature promoted microbial degradation, as indicated by decreases in the FLF only at the *Cassiope* site, but did not lead to changes in bacterial community compositions (Figures 3 and 4), which might be associated with the lack of significant differences in SOC molecular composition.

No significant differences in bacterial community structure and biomass in the litter and both soil layers were observed, although there was only a decrease in SOC content with warming at the *Cassiope* site (Figures 1, 3, and 4). There were several reports of no changes in bacterial community structure in response to warming (Allison, Wallenstein, & Bradford, 2010), and total soil microbial biomass previously investigated by chloroform fumigation-extraction at Zackenberg was unchanged by warming but higher in *Salix* than *Cassiope* heath (Blok et al., 2018). The duration of experimental warming may not be long enough to generate pronounced changes, or the bacterial community may be resilient to this low degree of increasing temperature (0.9°C). Zi et al. (2018) also reported no change in bacterial composition and diversity despite significant changes in extracellular enzyme activity. Thus, our DNA-based approach may not be a very compelling method to detect any probable changes in active microbial levels. In addition, this study did not investigate the fungal community, which can greatly contribute to the decomposition of organic matter (Wang et al., 2012). There are few studies of fungal and bacterial community composition in this high Arctic site, but the dominant plants in both heath types in Zackenberg associate with ericoid and ecto-mycorrhizal fungi that release enzymes that break down organic compounds (Michelsen, Quarmby, Sleep, & Jonasson, 1998).

4.3 | SOC stabilization mechanisms in Cryosol

Understanding SOC stabilization mechanisms in permafrost-affected soil is a very important issue, especially given the rapid climate change in the Arctic. Our study showed that more than 55% of SOC in the top 5-cm depth was associated with minerals, and this proportion increased as soil depth increased (Figure 1). Moreover, the C content in the HF and

silt+clay content showed a positive linear relationship under *Cassiope* (Figure S3). Thickening of the active layer as a result of warming may expose more mineral surfaces to mineral–organic matter interactions (Schuur & Mack, 2018). The higher proportion of silt and clay in soil may contribute to preserve SOC better through mineral–SOC interactions in the thawed layer. Furthermore, Gentsch et al. (2018) recently showed that organo-mineral associations could control decomposability and temperature sensitivity of SOC in permafrost soil. Thus, the high proportion of HF and C in the HF in both *Cassiope* and *Salix* soils indicated that mineral association could be an important SOC stabilization mechanism, and this may determine the fate of SOC in climate change scenarios in mineral-dominated Arctic soil. We found that the SOC for 5–10-cm depth in warmed plots was lower than in the control plots, which, as discussed above, might be due to different soil texture (Figure 1). This also emphasized the potential of preserving C with organo-mineral associations in Arctic soil (Gentsch et al., 2015; Gundelwein et al., 2007).

In our study, the mineral-associated HF showed more intense SOC transformation compared to the FLF: a lower C/N ratio and higher alkyl C to O/N alkyl C ratio in the HF (Tables 2 and 3). Whereas O/N alkyl C generally represents carbohydrates that are abundant in fresh plant materials, alkyl C is indicative of plant waxes, other aliphatic compounds or microbially resynthesized lipids (Marín-Spiotta, Swanston, Torn, Silver, & Burton, 2008). Thus, many studies showed that O/N alkyl C decreased and alkyl C increased as plant litter decomposed, and thus the alkyl C to O/N alkyl C ratio typically increases with decomposition (Kögel-Knabner, 1997; Preston, Nault, & Trofymow, 2009). Gentsch et al. (2015) also reported that mineral-associated organic matter showed characteristics of decomposition, such as a narrow C/N ratio, a higher $\delta^{13}C$ and $\delta^{15}N$ signature, and higher alkyl C to O/N alkyl C ratio than particulate organic matter. The C and N stable isotopes in decaying litter or organic matter were enriched during organic matter decomposition due to microbial kinetic discrimination or incorporation of microbial biomass/residues (Ågren, Bosatta, & Balesdent, 1996; Craine et al., 2015). These characteristics are indicative of more degraded organic matter in the HF than the LF and have been reported in numerous studies on temperate soils (Grandy & Neff, 2008). Proteins were more abundant in the HF than the other fractions in both soils (Table S5), and the C molecules associated with silt and clay size mineral particles represented more decomposed SOC characteristics with a higher alkyl C to O/N alkyl C ratio than the FLF (Table 3). Therefore, NMR-based characteristics and C/N ratio in the HF suggest that SOC–mineral association contains a large proportion of

microbially processed products (Gentsch et al., 2015; Gundelwein et al., 2007).

Another likely SOC stabilization mechanism could be aggregation. The relative mass proportion of the OLF was similar to that of the FLF and the aggregate-protected C pool (OLF-C) was more than 20% in the topsoil of *Cassiope* (Figure 1a). This contribution of the OLF to total SOC content was as high as in soils in temperate regions. John, Yamashita, Ludwig, and Flessa (2005) showed that 5.4–18.0% of SOC was stored in aggregates in agricultural, grassland and forest soil. The OLF-C pool in the *Salix* plot was also more than 10%, although one of its major components was charcoal/coal (Table S5). Charcoal/coal was likely to be windblown and deposited on the experimental site, possibly as particles from Mesozoic coal deposits. The aggregation in silt- and clay-dominated soil, such as under *Salix* heaths, may play a role in preserving charcoal/coal inside aggregates. The molecular C structure of the OLF showed that there were more chemically stable compounds such as charcoal and more microbially processed compounds than in the FLF, with a higher alkyl to O/N alkyl C ratio (Table 3). Restricting the accessibility of decomposers to SOC through aggregation has been suggested as an important mechanism to preserve SOC in temperate soil. However, studies on aggregate-protected C in the permafrost region are scarce (Mueller et al., 2015). Thus, further research should scrutinize several SOC stabilization mechanisms in permafrost-affected soils in detail.

5 | CONCLUSIONS

A number of studies on Arctic soils showed increased microbial activity and decomposition following increased temperature, and their results underscore feedback effects from SOC decomposition to global warming. Our study showed decreased SOC content under *Cassiope* exposed to long-term warming in the field experiment, and this was caused by increased decomposition in the FLF under warming. Although the FLF had the smallest contribution to total soil mass, changes in the FLF were large enough to cause the changes in total SOC. Thus, our study revealed the response of the light fraction of SOC to increased temperature and its great role in determining SOC storage in the high Arctic. On the other hand, there was no significant warming effect on *Salix* heath soil. Temperature increase was lower at the *Salix* site, perhaps because of different soil characteristics, such as higher moisture content, contributing to the absence of a warming effect on SOC under *Salix*. This implies that soil properties can influence the degree of soil warming and, thus, its effects on SOC. Furthermore, organic matter–mineral association may play a key role in determining SOC

stabilization and destabilization in mineral-dominated Arctic soils in a warming world.

CONFLICTS OF INTEREST

The authors have no conflicts of interest to declare.

DATA AVAILABILITY STATEMENT

Raw sequencing data were submitted to the NCBI Sequence Read Archive (SRA) with accession number PRJNA416693.

ORCID

Ji Young Jung https://orcid.org/0000-0003-4583-3957
Anders Michelsen https://orcid.org/0000-0002-9541-8658
Mincheol Kim https://orcid.org/0000-0003-1506-4800
Niels M. Schmidt https://orcid.org/0000-0002-4166-6218
Yoo Kyung Lee https://orcid.org/0000-0002-1271-5738

REFERENCES

Ågren, G. I., Bosatta, E., & Balesdent, J. (1996). Isotope discrimination during decomposition of organic matter: A theoretical analysis. *Soil Science Society of America Journal*, 60, 1121–1126.

Alatalo, J. M., Jägerbrand, A. K., Juhanson, J., Michelsen, A., & Ĺuptáčik, P. (2017). Impacts of twenty years of experimental warming on soil carbon, nitrogen, moisture and soil mites across alpine/subarctic tundra communities. *Scientific Reports*, 7, 44489. https://doi.org/10.1038/srep44489

Allison, S. D., Wallenstein, M. D., & Bradford, M. A. (2010). Soil-carbon response to warming dependent on microbial physiology. *Nature Geoscience*, 3, 336–340.

Biasi, C., Meyer, H., Rusalimova, O., Hämmerle, R., Kaiser, C., Baranyi, C., … Richter, A. (2008). Initial effects of experimental warming on carbon exchange rates, plant growth and microbial dynamics of a lichen-rich dwarf shrub tundra in Siberia. *Plant and Soil*, 307, 191–205.

Blok, D., Faucherre, S., Banyasz, I., Rinnan, R., Michelsen, A., & Elberling, B. (2018). Contrasting above- and belowground organic matter decomposition and carbon and nitrogen dynamics in response to warming in High Arctic tundra. *Global Change Biology*, 24, 2660–2672. https://doi.org/10.1111/gcb.14017

Campioli, M., Schmidt, N. M., Albert, K. R., Leblans, N., Ro-Poulsen, H., & Michelsen, A. (2013). Does warming affect growth rate and biomass production of shrubs in the high Arctic? *Plant Ecology*, 214, 1049–1058.

Craine, J. M., Elmore, A. J., Wang, L., Augusto, L., Baisden, W. T., Brookshire, E. N., … Zeller, B. (2015). Convergence of soil nitrogen isotopes across global climate gradients. *Scientific Reports*, 5, 8280. https://doi.org/10.1038/srep08280

Crowther, T. W., Todd-Brown, K. E. O., Rowe, C. W., Wieder, W. R., Carey, J. C., Machmuller, M. B., … Bradford, M. A. (2016). Quantifying global soil carbon losses in response to warming. *Nature*, 540, 104–108.

Elberling, B., Jakobsen, B. H., Berg, P., Søndergaard, J., & Sigsgaard, C. (2004). Influence of vegetation, temperature, and water content on soil carbon distribution and mineralization in four high Arctic soils. *Arctic, Antarctic, and Alpine Research*, 36, 528–538.

Eldridge, S. M., Chen, C. R., Xu, Z. H., Nelson, P. N., Boyd, S. E., Meszaros, I., & Chan, K. Y. (2013). Molecular composition of recycled organic wastes, as determined by solid-state ^{13}C NMR and elemental analyses. *Waste Management*, 33, 2157–2169.

Feng, X., Simpson, A. J., Wilson, K. P., Dudley Williams, D., & Simpson, M. J. (2008). Increased cuticular carbon sequestration and lignin oxidation in response to soil warming. *Nature Geoscience*, 1, 836–839.

Gee, W. G., & Or, D. (2002). Particle-size analysis. In J. H. Dane & G. C. Topp (Eds.), *Methods of soil analysis. Book series: 5. Part 4: Physical methods* (pp. 255–293). Madison, Wisconsin: Soil Science Society of America Inc.

Gentsch, N., Mikutta, R., Shibistova, O., Wild, B., Schnecker, J., Richter, A., … Guggenberger, G. (2015). Properties and bioavailability of particulate and mineral-associated organic matter in Arctic permafrost soils, Lower Kolyma Region, Russia. *European Journal of Soil Science*, 66, 722–734.

Gentsch, N., Wild, B., Mikutta, R., Capek, P., Diakova, K., Schrumpf, M., … Guggenberger, G. (2018). Temperature response of permafrost soil carbon is attenuated by mineral protection. *Global Change Biology*, 24, 3401–3415.

Grandy, A. S., & Neff, J. C. (2008). Molecular C dynamics downstream: The biochemical decomposition sequence and its impact on soil organic matter structure and function. *Science of the Total Environment*, 404, 297–307.

Guan, S., An, N., Zong, N., He, Y., Shi, P., Zhang, J., & He, N. P. (2018). Climate warming impacts on soil organic carbon fractions and aggregate stability in a Tibetan alpine meadow. *Soil Biology and Biochemistry*, 116, 224–236.

Gundelwein, A., Müller-Lupp, T., Sommerkorn, M., Haupt, E. T. K., Pfeiffer, E.-M., & Wiechmann, H. (2007). Carbon in tundra soils in the Lake Labaz region of arctic Siberia. *European Journal of Soil Science*, 58, 1164–1174.

Guo, L., Ping, C., & Macdonald, R. W. (2007). Mobilization pathways of organic carbon from permafrost to arctic rivers in a changing

climate. *Geophysical Research Letters*, *34*, L13603. https://doi.org/10.1029/2007GL030689

Höfle, S., Rethemeyer, J., Mueller, C. W., & John, S. (2013). Organic matter composition and stabilization in a polygonal tundra soil of the Lena Delta. *Biogeosciences*, *10*, 3145–3158.

Huang, J., Zhang, X., Zhang, Q., Lin, Y., Hao, M., Luo, Y., … Zhang, J. (2017). Recently amplified arctic warming has contributed to a continual global warming trend. *Nature Climate Change*, *7*, 875–879.

Hugelius, G., Strauss, J., Zubrzycki, S., Harden, J. W., Schuur, E. A. G., Ping, C. L., … Kuhty, P. (2014). Estimated stocks of circumpolar permafrost carbon with quantified uncertainty ranges and identified data gaps. *Biogeosciences*, *11*, 6573–6593.

IUSS Working Group WRB. (2015). *World reference base for soil resources 2014, update 2015: International soil classification system for naming soils and creating legends for soil maps*. Rome, Italy: FAO.

Jensen, L. M., & Rasch, M. (2013). *Zackenberg ecological research operations, 18th annual report 2012*. Roskilde, Denmark: Aarhus University.

John, B., Yamashita, T., Ludwig, B., & Flessa, H. (2005). Storage of organic carbon in aggregate and density fractions of silty soils under different types of land use. *Geoderma*, *128*, 63–79.

Klindworth, A., Pruesse, E., Schweer, T., Peplies, J., Quast, C., Horn, M., & Glockner, F. O. (2013). Evaluation of general 16S ribosomal RNA gene PCR primers for classical and next-generation sequencing-based diversity studies. *Nucleic Acids Research*, *41*, e1. https://doi.org/10.1093/nar/gks808

Kögel-Knabner, I. (1997). ^{13}C and ^{15}N NMR spectroscopy as a tool in soil organic matter studies. *Geoderma*, *80*, 243–270.

Marín-Spiotta, E., Swanston, C. W., Torn, M. S., Silver, W. L., & Burton, S. D. (2008). Chemical and mineral control of soil carbon turnover in abandoned tropical pastures. *Geoderma*, *143*, 49–62.

Michelsen, A., Quarmby, C., Sleep, D., & Jonasson, S. (1998). Vascular plant ^{15}N natural abundance in heath and forest tundra ecosystems is closely correlated with presence and type of mycorrhizal fungi in roots. *Oecologia*, *115*, 406–418.

Mueller, C. W., Rethemeyer, J., Kao-Kniffin, J., Löppmann, S., Hinkel, K. M., & Bockheim, J. G. (2015). Large amounts of labile organic carbon in permafrost soils of northern Alaska. *Global Change Biology*, *21*, 2804–2817.

Paré, M. C., & Bedard-Haughn, A. (2011). Optimum liquid density in separation of the physically uncomplexed organic matter in Arctic soils. *Canadian Journal of Soil Science*, *91*, 65–68.

Pisani, O., Hills, K. M., Courtier-Murias, D., Haddix, M. L., Paul, E. A., Conant, R. T., … Simpson, M. J. (2014). Accumulation of aliphatic compounds in soil with increasing mean annual temperature. *Organic Geochemistry*, *76*, 118–127.

Preston, C. M., Nault, J. R., & Trofymow, J. A. (2009). Chemical changes during 6 years of decomposition of 11 litters in some Canadian forest sites. Part 2. ^{13}C abundance, solid-state ^{13}C NMR spectroscopy and the meaning of "lignin". *Ecosystems*, *12*, 1078–1102.

Rozema, J., Weijers, S., Broekman, R., Blokker, P., Buizer, B., Werleman, C., … Cooper, E. (2009). Annual growth of *Cassiope tetragona* as a proxy for Arctic climate: Developing correlative and experimental transfer functions to reconstruct past summer temperature on a millennial time scale. *Global Change Biology*, *15*, 1703–1715.

Schirmer, M., Ijaz, U. Z., D'Amore, R., Hall, N., Sloan, W. T., & Quince, C. (2015). Insight into biases and sequencing errors for amplicon sequencing with the Illumina MiSeq platform. *Nucleic Acids Research*, *43*, e37. https://doi.org/10.1093/nar/gku1341

Schloss, P. D., Westcott, S. L., Ryabin, T., Hall, J. R., Hartmann, M., Hollister, E. B., … Weber, C. F. (2009). Introducing mothur: Open-source, platform-independent, community-supported software for describing and comparing microbial communities. *Applied and Environmental Microbiology*, *75*, 7537–7541.

Schmidt, N. M., Baittinger, C., & Forchhammer, M. C. (2006). Reconstructing century-long snow regimes using estimates of high Arctic *Salix arctica* radial growth. *Arctic, Antarctic, and Alpine Research*, *38*, 257–262.

Schnecker, J., Borken, W., Schindlbacher, A., & Wanek, W. (2016). Little effects on soil organic matter chemistry of density fractions after seven years of forest soil warming. *Soil Biology and Biochemistry*, *103*, 300–307.

Schrumpf, M., Kaiser, K., Guggenberger, G., Persson, T., Kögel-Knabner, I., & Schulze, E. D. (2013). Storage and stability of organic carbon in soils as related to depth, occlusion within aggregates, and attachment to minerals. *Biogeosciences*, *10*, 1675–1691.

Schuur, E. A. G., & Mack, M. C. (2018). Ecological response to permafrost thaw and consequences for local and global ecosystem services. *Annual Review of Ecology, Evolution, and Systematics*, *49*, 279–301.

Schuur, E. A. G., McGuire, A. D., Schadel, C., Grosse, G., Harden, J. W., Hayes, D. J., … Vonk, J. E. (2015). Climate change and the permafrost carbon feedback. *Nature*, *520*, 171–179.

Sistla, S. A., Moore, J. C., Simpson, R. T., Gough, L., Shaver, G. R., & Schimel, J. P. (2013). Long-term warming restructures Arctic tundra without changing net soil carbon storage. *Nature*, *497*, 615–618.

Six, J., Guggenberger, G., Paustian, K., Haumaier, L., Elliott, E. T., & Zech, W. (2001). Sources and composition of soil organic matter fractions between and within soil aggregates. *European Journal of Soil Science*, *52*, 607–618.

Sjögersten, S., van der Wal, R., & Woodin, S. J. (2012). Impacts of grazing and climate warming on C pools and decomposition rates in Arctic environments. *Ecosystems*, *15*, 349–362.

Soil Survey Staff. (2014). *Keys to soil taxonomy* (12th ed.). Washington, DC: USDA-Natural Resources Conservation Service.

Thaysen, E. M., Reinsch, S., Larsen, K. S., & Ambus, P. (2017). Decrease in heathland soil labile organic carbon under future atmospheric and climatic conditions. *Biogeochemistry*, *133*, 17–36.

von Lützow, M., Kögel-Knabner, I., Ekschmitt, K., Flessa, H., Guggenberger, G., Matzner, E., & Marschner, B. (2007). SOM fractionation methods: Relevance to functional pools and to stabilization mechanisms. *Soil Biology and Biochemistry*, *39*, 2183–2207.

Wang, H., He, Z., Lu, Z., Zhou, J., Van Nostrand, J. D., Xu, X., & Zhang, Z. J. (2012). Genetic linkage of soil carbon pools and microbial functions in subtropical freshwater wetlands in response to experimental warming. *Applied and Environmental Microbiology*, *78*, 7652–7661.

Wang, P., Heijmans, M. M. P. D., Mommer, L., van Ruijven, J., Maximov, T. C., & Berendse, F. (2016). Belowground plant biomass allocation in tundra ecosystems and its relationship with temperature. *Environmental Research Letters*, *11*, 055003. https://doi.org/10.1088/1748-9326/11/5/055003

Welker, J. M., Fahnestock, J. T., Henry, G. H. R., O'Dea, K. W., & Chimner, R. A. (2004). CO_2 exchange in three Canadian high Arctic ecosystems: Response to long-term experimental warming. *Global Change Biology*, *10*, 1981–1995.

Wickings, K., Grandy, A. S., Reed, S. C., & Cleveland, C. C. (2012). The origin of litter chemical complexity during decomposition. *Ecology Letters*, *15*, 1180–1188.

Wild, B., Gentsch, N., Čapek, P., Diáková, K., Alves, R. J. E., Bárta, J., … Richter, A. (2016). Plant-derived compounds stimulate the decomposition of organic matter in arctic permafrost soils. *Scientific Reports*, *6*, 25607. https://doi.org/10.1038/srep25607

Xu, X., Sherry, R. A., Niu, S., Zhou, J., & Luo, Y. (2012). Long-term experimental warming decreased labile soil organic carbon in a tallgrass prairie. *Plant and Soil*, *361*, 307–315.

Xu, X., Shi, Z., Li, D., Rey, A., Ruan, H., Craine, J. M., … Luo, Y. (2016). Soil properties control decomposition of soil organic carbon: Results from data-assimilation analysis. *Geoderma*, *262*, 235–242.

Xue, K., Yuan, M. M., Shi, Z. J., Qin, Y., Deng, Y., Cheng, L., … Zhou, J. Z. (2016). Tundra soil carbon is vulnerable to rapid microbial decomposition under climate warming. *Nature Climate Change*, *6*, 595–600.

Zhang, W., Jansson, P., Schurgers, G., Hollesen, J., Lund, M., Abermann, J., & Elberling, B. (2018). Process-oriented modeling of a high Arctic tundra ecosystem: Long-term carbon budget and ecosystem responses to interannual variations of climate. *Journal of Geophysical Research: Biogeosciences*, *123*, 1178–1196.

Zhang, X.-Z., Shen, Z.-X., & Fu, G. (2015). A meta-analysis of the effects of experimental warming on soil carbon and nitrogen dynamics on the Tibetan Plateau. *Applied Soil Ecology*, *87*, 32–38.

Zhao, Z., Dong, S., Jiang, X., Zhao, J., Liu, S., Yang, M. Y., … Sha, W. (2018). Are land use and short time climate change effective on soil carbon compositions and their relationships with soil properties in alpine grassland ecosystems on Qinghai-Tibetan Plateau? *Science of the Total Environment*, *625*, 539–546.

Zi, H. B., Hu, L., Wang, C. T., Wang, G. X., Wu, P. F., Lerdau, M., & Ade, L. J. (2018). Responses of soil bacterial community and enzyme activity to experimental warming of an alpine meadow. *European Journal of Soil Science*, *69*, 429–438.

SUPPORTING INFORMATION

Additional supporting information may be found online in the Supporting Information section at the end of this article.